Greenland meltwater as a significant and potentially bioavailable source of iron to the ocean

Maya P. Bhatia[1]*[†], Elizabeth B. Kujawinski[2], Sarah B. Das[3], Crystaline F. Breier[2], Paul B. Henderson[2] and Matthew A. Charette[2]*

The micronutrient iron is thought to limit primary productivity in large regions of the global ocean[1]. Ice sheets and glaciers have been shown to deliver bioavailable iron to the coastal and open ocean in the form of sediment released from the base of icebergs[2,3] and glacially derived dust[4]. More direct measurements from glacial runoff are limited, but iron concentrations are thought to be in the nanomolar range[5]. Here we present measurements of dissolved and particulate iron concentrations in glacial meltwater from the southwest margin of the Greenland ice sheet. We report micromolar concentrations of dissolved and particulate iron. Particulate iron concentrations were on average an order of magnitude higher than those of dissolved iron, and around 50% of this particulate iron was deemed to be potentially bioavailable, on the basis of experimental leaching. If our observations are scalable to the entire ice sheet, then the annual flux of dissolved and potentially bioavailable particulate iron to the North Atlantic Ocean would be approximately 0.3 Tg. This is comparable to dust-derived soluble iron inputs to the North Atlantic. We suggest that glacial runoff serves as a significant source of bioavailable iron to surrounding coastal oceans, which is likely to increase as melting of the Greenland ice sheet escalates under climate warming.

In Greenland, peak glacial runoff occurs at the height of the summer melt season when primary production in the North Atlantic has been limited by post-spring bloom nutrient depletion, and possible co-limitation with iron[6,7] (Fe). Previous studies indicate that aeolian Fe supply is not sufficient to support the maximum potential of primary productivity in the North Atlantic in the spring and summer[8,9]. Thus, glacial discharge of Fe from the Greenland ice sheet (GrIS) may support primary production in the North Atlantic Ocean during critical times of the year.

Much of the meltwater discharged from the GrIS drains from the surface (supraglacial) to the ice-sheet bed (subglacial), where it interacts with basal sediment and bedrock material before exiting at the base of land- and marine-terminating outlet glaciers[10,11]. Mechanical and chemical weathering beneath glaciers may produce nanoparticulate iron (oxyhydr)oxides from reactive iron-bearing phases under oxic conditions (for example, sulphides, carbonates, olivines and pyroxenes)[3]. Subglacial microbial activity may yield secondary Fe minerals that are more labile than the original silicate rock matrix, and thus supply dissolved Fe to the runoff waters[5]. Finally, the presence of organic ligands and Fe-reducing anoxic regions at the bed may serve to maintain a portion of the comminuted Fe in solution.

Here, we present dissolved and particulate Fe concentrations in glacial and proglacial runoff draining the GrIS. We measured dissolved Fe (hereafter dFe; $<0.2\,\mu m$) and Fe (oxyhydr)oxides in suspended sediments on $0.7\,\mu m$ filters (hereafter pFe) using inductively coupled plasma mass spectrometry (ICP-MS). The dFe fraction includes aqueous and nanoparticulate Fe, and may not be truly dissolved[3,12]. For the pFe, we used a $0.25\,M$ hydroxylamine hydrochloride in $0.05\,M$ hydrochloric acid leach to extract the amorphous (oxy)hydroxides of iron (adapted from previous work[13,14] as described earlier[15]; defined here as potentially bioavailable pFe), followed by a $1\,M$ hydroxylamine in 25% acetic acid leach to extract crystalline Fe (hydr)oxides (defined here as crystalline pFe). The Fe released from the sum of these leaches is defined as total (oxyhydr)oxides. Within the pFe fraction, the first leach procedure (Table 1) has the most implications for downstream Fe fertilization because it serves as our best approximation of the abundance and export of labile Fe. This pFe fraction is probably a mixture of various amorphous Fe mineralogical phases, and thus further processing (for example, biological or (photo)chemical) may be required to make certain components of this fraction truly bioavailable.

Sampling was conducted at a land-terminating Greenland outlet glacier system in 2008 (Fig. 1; ref. 16). This site is typical of many land-terminating regions along the GrIS western margin, where runoff from several outlet glaciers (named here N, M and O glaciers) collects in a large, seasonally ice-covered proglacial lake that empties into a fjord. For comparison, supraglacial, proglacial and groundwater endmember samples were collected from the surrounding region, as well as surface sea water in a fjord at a secondary field site (see Supplementary Methods).

Previously we described the subglacial drainage system evolution beneath N glacier, which we broadly extrapolate to the other glaciers in this system[17]. Briefly, the subglacial drainage system beneath N glacier seasonally evolves from a distributed system in early May where a large proportion ($\geq 49\%$) of the runoff is from delayed flow waters stored at the bed, to a channelized drainage system in late May (12–36% delayed flow contribution) and July (5–17% delayed flow contribution), in which the runoff is comprised of increasing amounts of supraglacial ice melt with limited basal contact[17].

Dissolved and particulate Fe concentrations for the endmember samples (supraglacial ice and groundwater), glacial runoff samples (N, M and O glacier streams, and waterfall stream), proglacial

1

Table 1 | Ranges of dissolved (<0.2 µm) and particulate (>0.70 µm) Fe concentrations measured in samples from the GrIS margin.

Sample type	n_d	Dissolved Fe range (µM)	n_p	Particulate Fe range (µM)		
				Total (oxyhydr)oxide Fe	% PB	% crystalline
Endmember samples						
Supraglacial ice	1	0.11	1	27.6	15.4	84.6
Groundwater	6	0.29–431	0	—	—	—
Runoff samples						
N glacier runoff	13	2.20–9.31	18	50.4–322	35.9–75.3, mean = 49.9	20.7–64.1, mean = 50.1
M glacier runoff	2	3.52–4.07	1	25.5	49.1	50.1
O glacier runoff	1	9.95	1	30.0	46.1	53.1
Waterfall stream	1	0.19	0	—	—	—
Proglacial samples						
Proglacial lake	2	4.81–5.21	1	278	44.5	55.5
Lake outflow	1	17.4	1	45.4	48.7	51.3
Fjord samples						
Glacial runoff in fjord	2	2.34–2.86	0	—	—	—
Fjord water	1	0.03	1	0.13	100	BDL

The range of percentage contributions from potentially bioavailable and crystalline fractions to the total (oxyhydr)oxide Fe is shown for all of the samples, and the average percentage of potentially bioavailable (PB) and crystalline contribution is also shown for the N glacier runoff. The fjord samples are from the secondary (northern) field site. The number of samples for each sample type (dissolved (d) and particulate (p)) is shown in the n column. Samples below our detection limit are indicated by BDL.
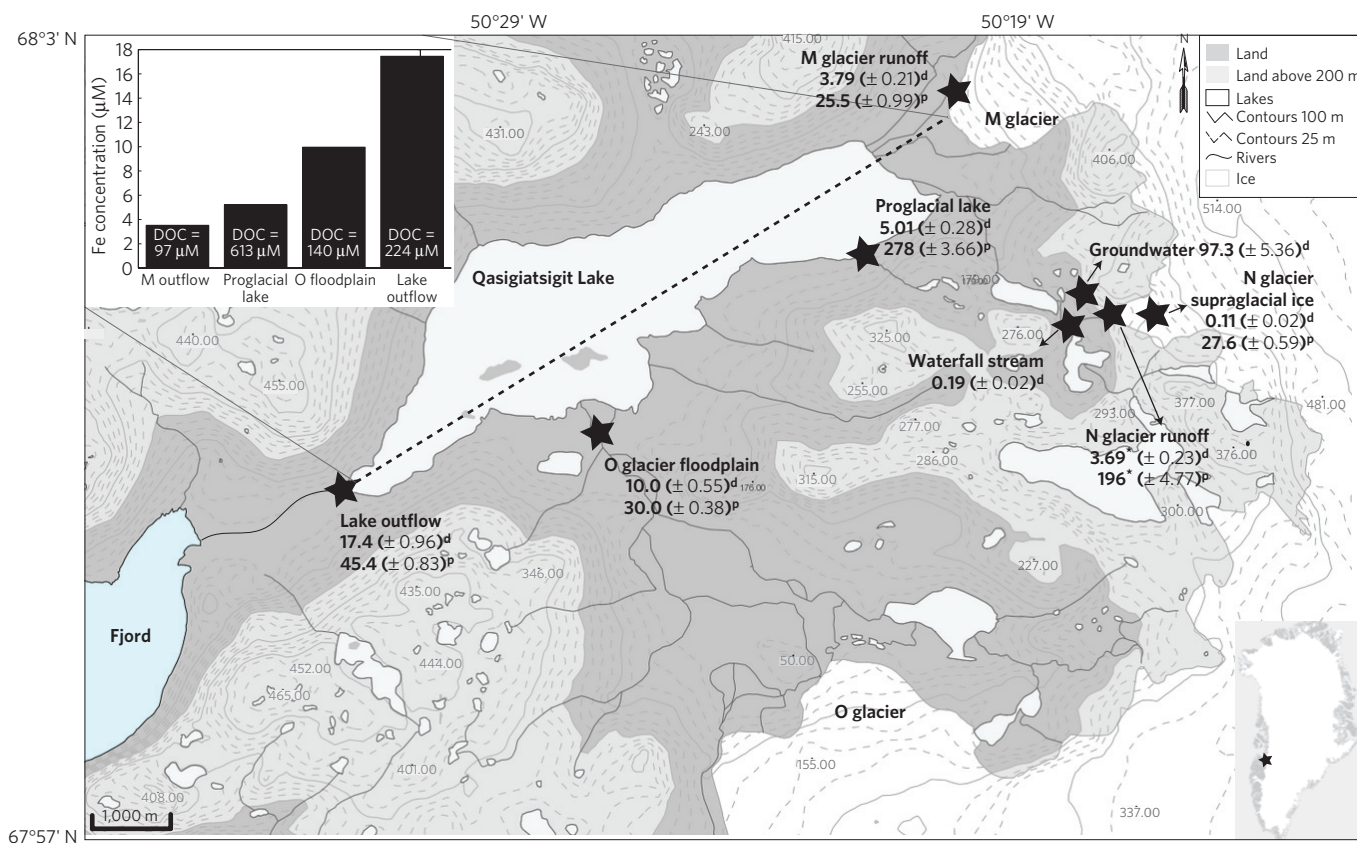

Figure 1 | Map of primary sample locations on the southwestern margin of the GrIS (1:100, adapted from NunaGIS). Approximate sample locations (black stars) are named in italic text, and contour elevations are shown in metres. Average dissolved (d; <0.2 µm) and particulate (oxyhydr)oxide (p; >0.7 µm) Fe concentrations and errors (±) in measurements are reported in micromolar concentrations. The N glacier runoff values (*) are discharge-weighted average concentrations. The dFe concentrations in samples along a transact (black dashed line) are plotted in the inset, with the DOC concentrations (previously reported in ref. 19) measured in each sample also shown.

samples (proglacial lake and lake outflow) and fjord samples are shown in Fig. 1 and Table 1, respectively. The seasonal discharge-weighted average dFe concentration for the N glacier runoff and the average dFe concentration from the adjacent, larger M glacier were similar (3.7 µM and 3.8 µM, respectively). This value is an order of magnitude higher than that previously reported for Greenland glacial discharge (dFe (<0.4 µm) = 54 nM; ref. 5), Antarctic basal ice (dFe (<0.2 µm) = 0.09–2.0 nM; ref. 2) and
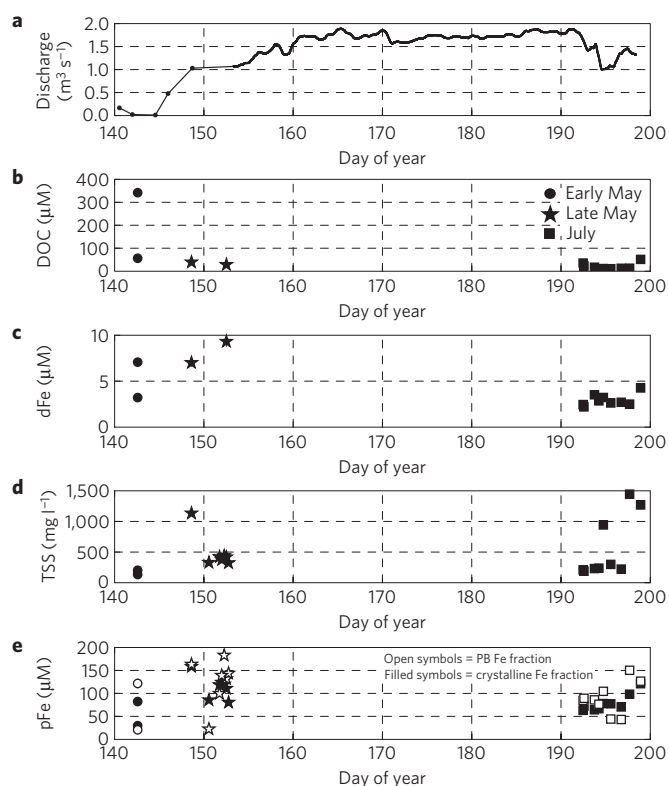
Figure 2 | Time series at N glacier. a, 24-h moving average discharge measured from 18 May to 16 July 2008, previously reported in ref. 17; the thin black line (days 140–153) indicates discontinuous discharge. **b,c**, Corresponding DOC concentrations (**b**) and dissolved Fe (dFe, <0.2 μm) concentrations (**c**) measured in the N glacier runoff. **d,e**, Corresponding total suspended sediment (TSS; **d**) and particulate Fe (pFe, >0.7 μm) concentrations (**e**) in the N glacier runoff. Error bars for all of the N glacier runoff Fe measurements are smaller than the data points.

average Arctic river dFe concentrations (Ob and Yenisey rivers (dFe < 0.4 μm): 251–654 nM; ref. 18).

The subglacially routed N and M glacial-runoff dFe concentrations were much higher than the dFe in the supraglacial ice (0.11 μM) and other supraglacially derived meltwater (0.19 μM; waterfall stream, see Supplementary Methods). This suggests that passage through the subglacial environment alters the dFe signature of glacial runoff relative to its origin as dilute ice melt. Furthermore, the higher-resolution time series at N glacier revealed seasonal variability, with the early season (May) runoff dFe concentrations (3.21–9.31 μM) being generally higher compared with the July runoff (2.20–4.26 μM). There are several potential controls on the dFe concentrations observed in the N glacier runoff. In our previous work at N glacier, we show that the subglacial drainage system probably accesses hypoxic or anoxic regions of the bed in the early season, particularly on the lowest discharge day[19]; under such conditions, Fe^{2+} is thermodynamically stable and would be transported passively into the glacier runoff[20]. Alternatively, one of the highest N glacier runoff dFe concentrations measured (7.06 μM) may be a result of the extremely high dissolved organic carbon (DOC) concentrations observed in these waters (~342 μM; Fig. 2), which can complex both ferrous (Fe^{2+}) and ferric (Fe^{3+}) iron in solution[21].

The pFe concentrations were higher for each sample type compared with the dFe concentrations (Fig. 1 and Table 1). This leachable pFe fraction lends insight into the Fe content of the underlying bedrock and sediment from which the dFe load in the runoff is ultimately derived. In the N glacier runoff, the pFe

concentrations in July may be entirely a function of the total suspended sediment (TSS) concentrations (model II geometric mean regression, $r^2 = 0.86$). However, in late May, when the highest pFe concentrations were observed, only the potentially bioavailable pFe fraction was well correlated with TSS ($r^2 = 0.69$), indicating that other hydrological or chemical controls on the Fe concentrations are also present. The pFe in the supraglacial ice endmember was primarily comprised of crystalline (non-labile) Fe (85%), compelling evidence that the potentially bioavailable pFe fraction (on average 50%) in the N glacier runoff results from physical, chemical and/or biological processes[3,21] occurring in the subglacial environment.

On the basis of results from samples collected in May, we propose that proglacial processing may add dissolved Fe to runoff originally exported at the glacier snout. In particular, processes in the proglacial lake (see Methods) increase dFe, whereas pFe decreases along the lake length (Fig. 1). This decoupling suggests that the lake dissolved and particulate Fe pools are controlled by separate mechanisms. The lake dFe concentration may be elevated in May (5.21 μM) because regions of the lake may be driven to anoxia beneath the seasonal ice cover, serving to maintain Fe^{2+} in solution. Furthermore, organic carbon concentrations were very high (~614 μM) in the lake in May (Fig. 1), and thus, Fe stabilization by organic ligands may also contribute to the high dFe concentrations[21]. Subsequently, the lower pFe concentrations in the lake outflow may be due to larger particles settling out along the length of the proglacial lake. The fact that the lake outflow has a similar ratio of potentially bioavailable pFe to crystalline pFe as the glacial samples suggests that the proglacial lake removes both labile Fe and crystalline Fe through aggregation and settling.

Although we lack a sample from the fjord at the end of this lake to investigate what portion of the Fe load ultimately is exported to the coastal ocean, samples collected from a fjord environment at a secondary site (albeit at a marine-terminating outlet glacier) are lower (Table 1), suggesting that a significant fraction of both the dissolved and particulate pools may be removed in the near coastal ocean[22]. In this way, glacial systems may be akin to river systems, where river Fe is generally depleted in estuaries before their entry into the marine environment through removal of the colloidal fraction by aggregation and deposition[22,23]. Although further transects from the ice-sheet terminus to the coastal ocean are needed to confirm this hypothesis, the dFe concentration (30 ± 20 nM) in the fjord water is similar to Arctic river (for example, Ob and Yenisey) estuary systems[18] but is orders of magnitude higher than the average dFe concentration in the ocean (0.7 nM; ref. 24). These observations hint that although a large proportion of the dissolved and particulate Fe load is removed, a comparatively significant fraction may still be exported to the coastal ocean.

Using the 2010 GrIS annual meltwater runoff[25], we estimate annual dFe and potentially bioavailable particulate Fe fluxes for the entire GrIS to be ~0.1 Tg yr^{-1} and 2.6 Tg yr^{-1}, respectively (see Methods for all calculations). In ref. 3, it was predicted that Fe in glacial meltwaters would probably be removed during estuarine transport, similar to riverine Fe. Assuming an estuarine removal factor of 90% (ref. 22), our dFe (<0.2 μm) flux equates to ~0.01 Tg yr^{-1}. For comparison, this value is an order of magnitude higher than that previously estimated for the GrIS (using a different filter pore size, dFe (<0.4 μm) ~ 0.001 Tg yr^{-1}; ref. 5) yet only an order of magnitude lower than the estimated annual global riverine dFe flux (dFe (< 0.45 μm) 0.14 Tg yr^{-1}; ref. 12). The combined dFe and potentially bioavailable pFe flux, after estuarine removal, is 0.3 Tg yr^{-1}. This total annual labile Fe flux from the GrIS is of the same order of magnitude as the annual soluble dust-derived Fe flux to the North Atlantic (0.07–0.7 Tg yr^{-1}; refs 26,27), which is generally believed to be the primary input of bioavailable Fe to this ocean[28].

Recently, it was reported[25] that most (~90%) of the freshwater flux from the GrIS is discharged into the North Atlantic Ocean, and that this flux has increased 136% from 1992 to 2010. Thus, the GrIS may be capable of providing a quantitatively significant portion of bioavailable Fe (and inorganic macronutrients)[19] in a buoyant plume to the surrounding North Atlantic, capable of stimulating primary productivity. This could explain recent results[29] showing a strong correlation between peak phytoplankton blooms off the coast of Greenland and GrIS runoff. Other factors such as buoyancy of the meltwater plume and further photochemical degradation and release of nanoparticulate Fe may allow the glacially derived Fe to remain within the euphotic zone of farther-afield marine waters. Icebergs may provide yet another source of glacially derived Fe to the North Atlantic, a mechanism shown to occur in the Southern Ocean[2] but not yet investigated around Greenland. This may be another significant, and underrepresented input, as solid ice discharge accounts for ~50% of the total GrIS freshwater flux at present[25]. GrIS meltwater flux is increasing, and 2012 set new records for GrIS mass loss[30]. Given that the Fe flux variability in this study was most sensitive to meltwater discharge, we would expect this glacial contribution of Fe to the North Atlantic Ocean to continue to increase under future warming scenarios.

Methods

Sample collection. All plastic-ware used in Fe sample collection and analysis was cleaned as follows: MilliQ rinse followed by a 5-day soak in 0.1% citronox, 7× rinse with MilliQ, 5-day soak in 10% HCl, and a final 3× MilliQ rinse. Plastic-ware cleaning was done in a designated (class 100) trace-metal clean laboratory. Hereafter we refer to this procedure as trace-metal cleaned. All solvents used for cleaning and sample analysis were Optima trace-metal grade or better.

For the dissolved samples, glacial meltwater was collected directly from the streams/ponds using new trace-metal cleaned 60 ml plastic syringes and 0.2 μm Sterivex filters (Millipore). Filters were rinsed with a full syringe volume of sample before collection. Filtered samples were stored in trace-metal cleaned 20 ml low-density polyethylene bottles spiked with ~40 μl of 8 N nitric acid at room temperature until analysis. Particulate samples were collected on pre-weighed, combusted 0.7 μm glass fibre filters (GF/Fs) using a combusted glass filtration apparatus.

Leachable particulate Fe. The concentrations of the Fe (oxyhydr)oxides in the suspended sediments on a weighed fraction of the GF/F (0.7 μm; particulate Fe) were determined using the selective dissolution protocol described previously[15]. The only modification was that the leach and sediments were centrifuged post-leach in HDPE centrifuge tubes to ensure no sediment contamination during liquid sampling. This extraction has been shown to quantitatively extract ferrihydrite ($\gtrsim$45%) with minimal ($\lesssim$< 1%) dissolution of goethite and haematite[13]. However, previously cited caveats[15] regarding the difficulty in quantifying the specific Fe fractions dissolved by each leach are applicable here. Thus, the type of Fe extracted in different dissolution leaches is probably quite broad and the results are method-dependent. To constrain our results, we extracted Fe from a marine sediment reference standard (MESS-3, National Research Council of Canada) using the L3 and L4 leaches. Among four replicates, our total percentage of recovery for the MESS-3 standard ranged between 62 and 69% after the L4 leach; this provides context for the amount of total Fe recovered by our operationally defined Fe leaches from typical sediments. Aliquots of the L3 and L4 samples were diluted with 5% nitric acid (~1:20–1:600) before analyses.

ICP-MS analysis and blank corrections. Dissolved and particulate Fe was measured using a Thermo-Electron Element 2 high-resolution single collector ICP-MS, run in medium-resolution mode for ^{56}Fe. Aliquots of the dissolved and particulate samples were diluted and spiked with an internal standard solution (5% nitric acid, 3 ppb ^{115}In) to correct for instrument drift. Fe standards (also ^{115}In spiked) were prepared from a stock solution created from a certified 1,000 ppm reference standard (Specpure, AlfaAeser).

Sample concentrations were corrected for possible contributions from materials and filters by measuring process blanks. For the dissolved samples, the average Fe concentration of four MilliQ-water samples (0.0207 μM) processed in the laboratory analogously to the field samples was subtracted from the final measured sample Fe concentrations. Three further blanks were processed in the laboratory by filtering MilliQ water with syringes and Sterivex filters, as done in the field. However, the Fe concentrations in these laboratory process blanks were extremely low, less than the mean $HNO_3 - {}^{115}$In blank run on the ICP-MS. The relative standard deviation between our measured value of a certified

river water reference material (SLRS-5, NRC) over repeated measurements (1,961 ± 107 nmol kg^{-1}) and the reported value (1,844 ± 90 nmol l^{-1}) was 5.5%. This value was used with the standard deviation among the process blanks to determine the propagated error in each of our sample measurements. The average dFe error (μM) in the different samples (Fig. 1), and in each of the N glacier runoff samples (Fig. 2) is shown.

For the particulate samples, fractions of several pre-weighed, combusted GF/Fs prepared identically to those used for the samples were processed using the sequential L3 and L4 leaches. The average total GF/F L3/L4 leach blank (L3: 5.06×10^{-6} g; L4: 1.31×10^{-5} g) was then multiplied by the sample filter fraction and subtracted from the measured Fe concentration of the filter fraction for each leach. Generally, the GF/F leach blanks were low relative to the amount of Fe from the sample for both the L3 (average: 0.81 ± 1.28% and range: 0.06–7.85% of the total (oxyhydr)oxide Fe) and L4 (average: 1.7 ± 1.95% and range: 0.11–1.95% of the total (oxyhydr)oxide Fe). The only sample with a significant blank correction (41.2%) was from the fjord site. This value is not used in our flux calculations and therefore does not have an impact on the conclusions in this paper. The propagated error on our particulate measurements was done as above for the dissolved samples except that we used the relative standard deviation for each sample from the ICP-MS. The average total pFe error (μM) in the different samples (Fig. 1), and in the L3 and L4 leaches in each of the N glacier runoff samples (Fig. 2) is shown.

References

1. Moore, J. K., Doney, S. C., Glover, D. M. & Fung, I. Y. Iron cycling and nutrient-limitation patterns in surface waters of the World Ocean. *Deep Sea Res. II* **49,** 463–507 (2001).
2. Raiswell, R., Benning, L. G., Tranter, M. & Tulaczyk, S. Bioavailable iron in the Southern Ocean: The significance of the iceberg conveyor belt. *Geochem. Trans.* **9,** http://dx.doi.org/10.1186/1467-4866-9-7 (2008).
3. Raiswell, R. *et al.* Contributions from glacially derived sediment to the global iron (oxyhydr)oxide cycle: Implications for iron delivery to the oceans. *Geochim. Cosmochim. Acta* **70,** 2765–2780 (2006).
4. Crusius, J. *et al.* Glacial flour dust storms in the Gulf of Alaska: Hydrologic and meteorological controls and their importance as a source of bioavailable iron. *Geophys. Res. Lett.* **38,** L06602 (2011).
5. Statham, P. J., Skidmore, M. & Tranter, M. Inputs of glacially derived dissolved and colloidal iron to the coastal ocean and implications for primary productivity. *Glob. Biogeochem. Cycles* **22,** GB3013 (2008).
6. Blain, S., Guieu, C., Claustre, H. & Leblanc, K. Availability of iron and major nutrients for phytoplankton in the northeast Atlantic Ocean. *Limnol. Oceanogr.* **49,** 2045–2104 (2004).
7. Mills, M. M., Ridame, C., Davey, M., La Roche, J. & Geider, R. J. Iron and phosphorus co-limit nitrogen fixation in the eastern tropical North Atlantic. *Nature* **429,** 292–294 (2004).
8. Moore, C. M. *et al.* Iron limits primary productivity during spring bloom development in the central North Atlantic. *Glob. Change Biol.* **12,** 626–634 (2006).
9. Nielsdottir, M. C., Moore, C. M., Sanders, R., Hinz, D. J. & Achterberg, E. P. Iron limitation of the postbloom phytoplankton communities in the Iceland Basin. *Glob. Biogeochem. Cycles* **23,** GB3001 (2009).
10. Bartholomew, I. *et al.* Seasonal evolution of subglacial drainage and acceleration in a Greenland outlet glacier. *Nature Geosci.* **3,** 408–411 (2010).
11. Das, S. B. *et al.* Fracture propagation to the base of the Greenland Ice Sheet during supraglacial lake drainage. *Science* **320,** 778–781 (2008).
12. Raiswell, R. & Canfield, D. E. The iron biogeochemical cycle past and present. *Geochem. Perspect.* **1,** 1–220 (2012).
13. Chao, T. T. & Zhou, L. Extraction techniques for selective dissolution of amorphous iron-oxides from soils and sediments. *Soil Sci. Soc. Am. J.* **47,** 225–232 (1983).
14. Hall, G. E. M., Vaive, J. E., Beer, R. & Hoashi, M. Selective leaches revisited, with emphasis on the amorphous Fe oxyhydroxide phase extraction. *J. Geochem. Explor.* **56,** 59–78 (1996).
15. Charette, M. A., Sholkovitz, E. R. & Hansel, C. M. Trace element cycling in a subterranean estuary: Part 1. Geochemistry of the permeable sediments. *Geochim. Cosmochim. Acta* **69,** 2095–2109 (2005).
16. Escher, A. *Geological Maps of Greenland 1:500,000* (Geological Survey of Denmark and Greenland (GEUS), 1971).
17. Bhatia, M. *et al.* Seasonal evolution of water contributions to discharge from a Greenland outlet glacier: Insight from a new isotope-mixing model. *J. Glaciol.* **57,** 929–941 (2011).
18. Dai, M. H. First data on trace metal level and behaviour in two major Arctic river-estuarine systems (Ob and Yenisey) and in the adjacent Kara Sea, Russia. *Earth Planet. Sci. Lett.* **131,** 127–141 (1995).
19. Bhatia, M., Das, S. B., Xu, X. L., Charette, M. & Kujawinski, E. B. Organic carbon export from the Greenland ice sheet. *Geochim. Cosmochim. Acta* http://dx.doi.org/10.1016/j.gca.2013.02.006 (in the press, 2013).

20. Achterberg, E. P., Holland, T. W., Bowie, A. R., Mantoura, R. F. C. & Worsfold, P. J. Determination of iron in seawater. *Anal. Chim. Acta* **442,** 1–14 (2001).
21. Rue, E. L. & Bruland, K. W. The role of organic complexation on ambient iron chemistry in the equatorial Pacific Ocean and the response of a mesoscale iron addition experiment. *Limnol. Oceanogr.* **42,** 901–910 (1997).
22. Boyle, E. A., Edmond, J. M. & Sholkovitz, E. R. The mechanism of iron removal in estuaries. *Geochim. Cosmochim. Acta* **41,** 1313–1324 (1977).
23. Wen, L-S., Santschi, P., Gill, G. & Paternostro, C. Estuarine trace metal distributions in Galveston Bay: Importance of colloidal forms in the speciation of the dissolved phase. *Mar. Chem.* **63,** 185–212 (1999).
24. Sarmiento, J. & Gruber, N. *Ocean Biogeochemical Dynamics* (Princeton Univ. Press, 2006).
25. Bamber, J., van den Broeke, M., Ettema, J., Lenaerts, J. & Rignot, E. Recent large increases in freshwater fluxes from Greenland into the North Atlantic. *Geophys. Res. Lett.* **39,** L19501 (2012).
26. Boyd, P. W., Mackie, D. S. & Hunter, K. A. Aerosol iron deposition to the surface ocean—Modes of iron supply and biological responses. *Mar. Chem.* **120,** 128–143 (2010).
27. Fan, S. M., Moxim, W. J. & Levy, H. Aeolian input of bioavailable iron to the ocean. *Geophys. Res. Lett.* **33,** LO7602 (2006).
28. Jickells, T. D. *et al.* Global iron connections between desert dust, ocean biogeochemistry, and climate. *Science* **308,** 67–71 (2005).
29. Frajka-Williams, E. & Rhines, P. B. Physical controls and interannual variability of the Labrador Sea spring phytoplankton bloom in distinct regions. *Deep-Sea Res. I* **57,** 541–552 (2010).
30. Tedesco, M. *et al.* Evidence and analysis of 2012 Greenland records from spaceborne observations, a regional climate model and reanalysis data. *Cryos. Discuss.* **6,** 4939–4976 (2012).

Acknowledgements

Author contributions

M.P.B., E.B.K., S.B.D. and M.A.C. designed the research. M.P.B., E.B.K., P.B.H. and M.A.C. collected the samples. M.P.B. and C.F.B. analysed the samples. M.P.B. and M.A.C. analysed the data. M.P.B., E.B.K., S.B.D. and M.A.C. wrote the paper.

Additional information

Supplementary information is available in the online version of the paper. Reprints and permissions information is available online at www.nature.com/reprints. Correspondence and requests for materials should be addressed to M.P.B. or M.A.C.

Competing financial interests

The authors declare no competing financial interests.